

Biodegradable Biodevices: A Design Approach Based on Cellular Automaton

William Solórzano-Requejo^a, Carlos Aguilar^b, Gabriel Callejo and Andrés Díaz Lantada^c
Department of Mechanical Engineering, ETSI Industriales, Universidad Politécnica de Madrid,
c/ José Gutiérrez Abascal 2, 28006 Madrid, Spain

Keywords: Biodegradable Medical Devices, Biodegradable Materials, Degradation Modelling, Simulation of Medical Devices, Cellular Automata.

Abstract: This innovative study introduces a comprehensive methodology to simulate the two-dimensional degradation of biodegradable materials, a crucial aspect in biodevice design. Several PVA specimens of diverse shapes were created, and their degradation was computationally modelled using cellular automaton. Deterministic and probabilistic transition rules were explored to identify the most accurate in the simulation of PVA degradation. The results highlight the effectiveness of the probabilistic exponential rule, derived from Markov Chains, for reliable degradation simulation. Furthermore, this approach was successfully applied to the analysis of specific medical devices, enabling a detailed *in silico* assessment of degradation patterns in coronary stents, tissue engineering scaffolds and craniostylosis implants. This methodology deepens our fundamental understanding of degradation and provides valuable information for engineers and medical professionals, facilitating the creation of devices that integrate optimally with surrounding biological tissues.

1 INTRODUCTION

Cellular automaton (CA) are discrete, local dynamical systems that can be considered in several ways: as a mathematical idealization of natural systems, a discrete caricature of microscopic dynamics, a parallel algorithm, or a discretization of partial differential equations. From an engineering perspective, CAs are networks composed of finite-state machines, also known as cells, that operate through localized interactions. These cells evolve collectively, and the evolution of the system is determined by the interaction of their individual components (Dascălu, 2018).

In essence, CAs are conceptualized as sets of cells arranged in grids. Over sequential steps or iterations, these grids are dynamically transformed according to specific predefined rules. During these iterations, the state of each cell changes, influenced by both the predetermined rules and the previous states of neighbouring cells. If all cells are updated simultaneously, the automaton is called synchronous.

On the other hand, if only one cell is updated per iteration, it is called asynchronous (Agapie et al., 2014; Dascălu, 2018).

Furthermore, CA can vary in terms of randomness. A deterministic automaton has no randomness; the evolution of the cells strictly follows predetermined rules. However, if the cell to be updated is chosen randomly and/or the local transition rule involves probabilities, the automaton is classified as probabilistic (Agapie et al., 2014; Dascălu, 2018).

In the 1950s, Konrad Zuse, Stanislav Marcin Ulam and John von Neumann formulated the first theories of CA in their strictest sense (Deutsch & Dormann, 2017). These pioneers used CA to model real-world phenomena, and von Neumann was particularly inspired by the self-reproduction capability observed in biological organisms (Von Neumann & Burks, 1966). His fascination with the inherent ability of living entities to create similar beings led him to explore artificial life. This exploration laid the foundation for the emergence of artificial life as a distinct field of study, connecting it

^a <https://orcid.org/0000-0002-2989-9166>

^b <https://orcid.org/0000-0003-0291-3041>

^c <https://orcid.org/0000-0002-0358-9186>

with artificial intelligence and genetic algorithms. These disciplines share a common thread of natural inspiration, as each replicates certain characteristics or constructive principles found in natural systems (Dascălu, 2018).

In 1970, John Conway presented the Game of Life automaton, a seemingly simple but profoundly meaningful representation of the processes of birth and death. This creation quickly became an icon in the field of CA, capturing the public imagination with its easily understood rules and captivating simulations. The Game of Life demonstrated the extraordinary ability of minimal, localized rules to generate intricate, self-organizing patterns (Gardner, 1970). It served as a paradigmatic example of the fundamental concept underlying CA: a basic, regular structure capable of giving rise to a wide variety of phenomena, even from initially chaotic states.

CA has been widely applied in diverse fields to model dynamical systems that exhibit organized behaviour, including areas such as statistical physics, biology, medicine, ecology, and socioeconomic interactions (Agapie et al., 2014). Interestingly, CAs have also found utility in the medical device design process. These automata have been used to represent a patient's mental state by integrating information from electroencephalogram analysis (Colafoglio et al., 2023), for neuronal image segmentation (Kalkhof et al., 2023), simulation of cells colonizing tissue engineering scaffolds (Díaz Lantada et al., 2023), optimization of biomimetic cell culture systems (Ballesteros Hernando et al., 2019), and even metamaterial design (Z. Liu et al., 2023).

Regarding the design of biodegradable and bioabsorbable implants made from polymers or metals, it is crucial to understand and quantify the degradation of the material and how its behaviour affects the biodesign. In this context, this article delves into the detailed explanation of a methodology that uses CA to two-dimensionally model the degradation of polymeric specimens.

2 MATERIALS AND METHODS

2.1 Test Bench and Specimens

To investigate the influence of neighbourhood on CA dynamics, various test specimens were utilized, including circular, triangular, hexagonal, quadrilateral, D and 4-shape geometries (Figure 1), all with maximum dimensions of 30 x 30 x 2 mm for the analysis of their two-dimensional degradation.

These probes were designed using Autodesk® Fusion 360 (Autodesk Inc., San Rafael, CA, USA).



Figure 1: PVA test specimens.

For the fabrication of the samples, Poly (vinyl alcohol) (PVA) was chosen as the material due to its rapid solubility in water, which facilitated the testing process outlined in this research. This thermoplastic material was purchased from Smart Materials 3D (Pol. Ind. El Retamar, c/ Tomillo 7, 23680 Alcalá la Real, Jaén, Spain) in form of monofilaments with a 1.75 mm diameter. The specimens were manufactured using fused deposition modelling (FDM), employing a Bambu Lab X1 Carbon Combo 3D printer equipped with a 0.4 mm diameter hardened steel nozzle.

To generate the tool path for printing, Bambu Studio (Austin, TX, USA), an open-source slicing software based on Prusa Slicer, was employed. The print parameters were consistently configured for all printed specimens: a layer thickness of 0.2 mm, a print speed of 40 mm/s, a bed temperature of 50 °C, a nozzle temperature of 220 °C, two perimeters, and a 100% rectilinear infill pattern.

To investigate degradation, a 12.0-megapixel high-resolution optical sensor with an f/1.5 lens and an optical photo stabiliser was used to capture test images at regular one-minute intervals and merge them all into a video. To ensure consistent results and avoid localised degradation, the samples were carefully placed inside a glass container, proportionally submerged in water. To prevent water ingress from the top to the bottom, PETG discs were used. This ensures that the degradation is two-dimensional, specifically from the sides of the specimen. The container was filled with 600 mL of water, and maintained at a constant temperature of 27°C.

2.2 Image Processing

Frames were extracted from the video of each experiment, revealing the appearance of bubbles due to specimen degradation. Subsequently, it was necessary to segment the PVA specimen, as this segmentation allowed defining the CA transition rules. To distinguish between the background, the bubbles and the PVA in each frame, the K-Means algorithm was used. This unsupervised algorithm analysed the unlabelled image and grouped pixels

with similar characteristics. The result was a mask divided into 3 zones ($K = 3$). Unfortunately, K-Means was insufficient to extract the degraded PVA, so it was complemented with Morphological Geodesic Active Contour (MGAC). MGAC is especially suitable for images with visible contours, even in cases where these contours are noisy, cluttered, or partially blurred, however, it requires preprocessing to highlight these contours (Caselles et al., 1997). In this case, K-Means segmentation was used to highlight the contours, penalizing the areas belonging to the background and the bubbles by multiplying their pixel values by 0 and 0.5 respectively, and highlighting the region with degraded material by preserving their pixel values (Figure 2). In addition, all images were aligned by changing their perspective to avoid deformations that may result in erroneous compression of the degradation. This whole process was done in Python[®] 3.7.14 (Python Software Foundation) using OpenCV and scikit-image libraries.

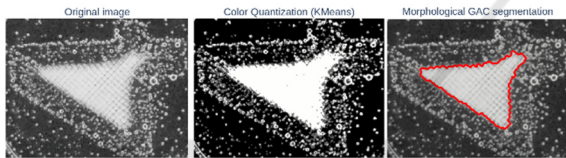


Figure 2: Image processing steps.

2.3 Cellular Automaton

CA is specified by a grid composed of cells, a set of states characterizing the cells (ε), an interaction neighbourhood (\mathcal{N}) and a rule (R) which determines the dynamics (Deutsch & Dormann, 2017). To model the degradation of PVA samples, it is necessary to define all these parameters since the complexity of the model depends on them. Moreover, the higher generality of the probabilistic CA (PCA) makes this model more efficient compared to the deterministic one (Agapie et al., 2014). In the following subsections, each of the components of the CA will be explained in detail.

2.3.1 Grid, Boundary Condition and States

A grid, denoted \mathcal{L} , is composed of a set of cells represented by r . This grid \mathcal{L} establishes the spatial framework in which the automaton operates and can assume a finite or infinite nature. In our model, the CA grid is the initial already processed grayscale image captured after the experiments performed on each sample (Figure 3A).

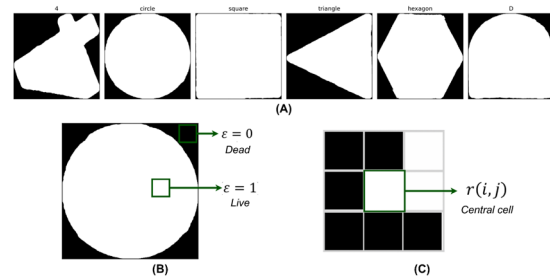


Figure 3: (A) Grids, (B) states and (C) neighbourhood of the CA model.

In this scenario, the cells correspond to individual pixels of the image. This discrete spatial representation is crucial for CAs. In this case it is possible to quantify the pixel dimensions, each pixel measuring $50 \times 50 \mu\text{m}$. This accurate spatial analysis is essential in the computational framework, because if the pixel size dimensions change, the transition rules could differ, and the model would have to be recalibrated.

The CA model has two states: "live" ($\varepsilon = 1$), which indicates the presence of PVA material in the cell, and "dead" ($\varepsilon = 0$), which indicates the absence of material or the presence of water causing PVA degradation (Figure 3B). This simplifies the complexity of the model, as it only considers these two states.

Since the CA mesh is finite, it is necessary to impose boundary conditions that specify the interaction neighbourhood of the cells at the boundary of the mesh. That boundary can be periodic, implying that the mesh is closed, reflective, the state of the cells at the mesh boundary is replicated, or fixed, one state is defined for the entire boundary. In this case, the fixed boundary was chosen and defined with the dead state because it favours material degradation.

2.3.2 Neighbourhood and Rule

An interaction neighbourhood $\mathcal{N}(r)$ defines the cells that impact the state dynamics of a specific cell $r(i, j) \in \mathcal{L}$. In two-dimensional CA, two prevalent types of neighbourhoods are widely used: the von Neumann neighbourhood, encompassing the four neighbouring cells along the vertical and horizontal axes, and the Moore neighbourhood (\mathcal{N}_M) comprising both side neighbours and corner cells. When considering degradation processes, all surrounding cells influence the degradation of the central cell ($r(i, j)$), leading to the incorporation of the Moore neighbourhood in CA degradation models (Figure 3C). This choice reflects the comprehensive influence of adjacent and diagonal cells on the degradation

dynamics of the focal cell, providing a more accurate representation of the system's behaviour.

$$\mathcal{N}_M(i, j) = \left\{ \begin{array}{l} r(i+1, j), r(i+1, j+1), r(i, j+1), \\ r(i-1, j+1), r(i-1, j), r(i-1, j-1), \\ r(i, j-1), r(i+1, j-1) \end{array} \right\} \quad (1)$$

The rule can be probabilistic or deterministic. The deterministic approach is simple: if a neighbouring cell is dead, the central cell will be dead in that iteration. In contrast, PCA introduces complexity. According to this scenario, if n cells surrounding the central cell are dead, there is a chance of degradation with a probability of P_n . Clearly, as the number of degraded cells around the central cell increases, the probability of going from a living to a dead state increase. How to obtain the probabilities in each case is detailed in the Results section. Furthermore, in the CA degradation model, all cells are updated simultaneously, so it is a synchronous automaton.

3 RESULTS

3.1 Modelling of PVA Specimens

In the Materials and Methods section, all the parameters involved in the creation of the CA for modelling the degradation of the PVA were described, except the rule that regulates the dynamics of the system. In this case, it is interesting to compare the deterministic approach with the probabilistic one; the latter requires the transition probabilities as a function of the neighbourhood, but because the current state is the only one responsible for the next state, CA becomes the perfect candidate for using Markov Chains (MC) to regulate the probabilities (Agapie et al., 2014).

First, it is important to understand the degradation phenomena. For this purpose, an analysis of the evolution of living pixels was carried out. Figure 4A summarises the decreasing exponential trend of the live pixels over time. To determine whether the degradation rate is constant or not, the scale was changed to exponential, and the number of live pixels was normalised (Figure 4B). This graph demonstrates two important aspects: the degradation rate is not constant, and the geometry of PVA specimens influences the degradation process because similar shapes exhibit almost the same degradation rate. For this reason, circular, triangular, and hexagonal specimens were chosen to apply the MC model and obtain the transition matrix, which defines the probabilities of the CA.

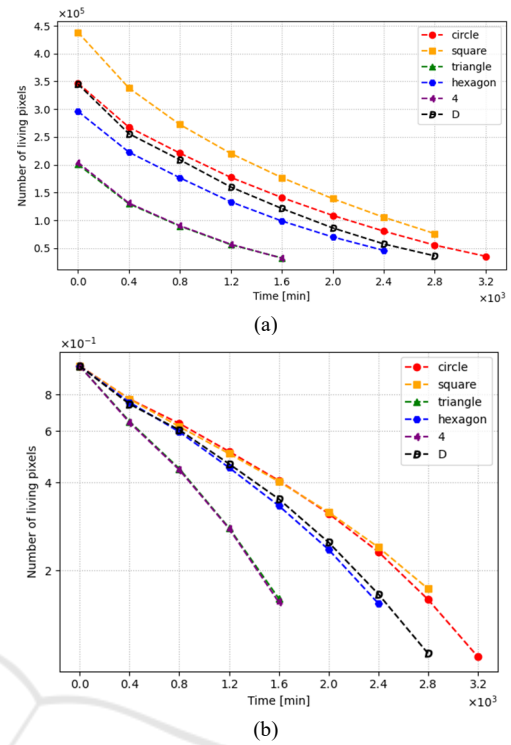


Figure 4: Graphical representation of living pixel dynamics, showing (A) dimensional and (B) dimensionless data.

MCs are stochastic processes characterised by a finite set of states. For these processes, the transition probabilities between states, denoted as p_{ij} , depend exclusively on the current state of the system. These probabilities are organised in a positive square transition matrix $P = (p_{ij})_{i,j=\overline{1,n}}$. In this context, the "dead" state ($\varepsilon = 0$) is absorbing, since once the system enters this state ($p_{00} = 1$), it can never leave.

By calculating the p_{10} transition probability from the ratio of the total number of cells to live cells, it is evident that this MC is heterogeneous because the transition matrix changes over time.

Therefore, the average value of the live-to-dead transition probability was calculated for each of the samples under study, considering only their degradation information every 400 minutes until the system is 80% degraded. Since the average transition probability is 0.254, the following rule is established: if the central cell is surrounded by at least one dead cell, the degradation probability is 0.254 (R_{det}). In addition, using the standard deviation information, two probabilities were calculated: 0.17 and 0.41. Two additional rules are defined considering that the probability follows an exponential (R_{exp}) or linear (R_{linear}) function, with 0.17 corresponding to the

probability of degradation if one of the neighbouring cells is dead and 0.41 if six cells are dead.

In addition, two other rules are established using linear ($R_{linear_01_09}$) and exponential distributions ($R_{exp_01_09}$). The probability starts at 0.1 when one of the cells is degraded and increases to 0.9 when six of them are degraded. It is important to note that when there are six degraded neighbours, it means that the cell is attached to the specimen only by one live pixel, and if there are seven dead cells, it implies that this pixel is isolated. In both cases, it is determined that the central cell will be degraded in that iteration. Furthermore, all these rules are compared with the deterministic one (R_{det}), which establishes that if at least one of the neighbours is degraded, the central cell will also be degraded. The whole CA was programmed in Python[®] and the rules were applied if the central cell is alive and if the transition probability, which depends on the number of dead neighbours, is greater than a random number.

Figure 5 compares the images obtained from the experiments with the simulations of the CA with the different rules. To determine the similarity between the experimental images and those obtained through the simulation, the mean square error (MSE) metric was used, then, the iteration that presented the highest similarity with the image of the degraded PVA specimen at each moment was selected. This metric also allowed us to quantify which of the rules provides the most morphologically reliable simulation. From the information provided by Figure 5 and the MSE analysis, it is concluded that the exponential rule (R_{exp}) obtained from the information found in the Markov chain is the most reliable.

3.2 Simulation of Medical Devices Degradation

Biodegradable implants offer several advantages for medical professionals. First, they eliminate the need for a second surgical intervention for removal, which saves time and resources. In addition, biodegradation can offer other significant advantages, for example, rigid, non-biodegradable titanium implants can cause problems such as refractures when removed, as the bone has not been able to bear sufficient load during the healing process. In contrast, biodegradable implants can degrade slowly, gradually transferring the load to the healing bone.

In tissue engineering, biodegradable scaffolds are essential to provide adequate mechanical support for damaged tissue and degrade gradually as new tissue

grows. However, the challenge lies in finding materials with specific mechanical properties and degradation rates for different tissues, as well as being able to fabricate customized scaffolds with precise pore interconnections (Y.-Y. Liu et al., 2023).

For coronary stents, a meticulous approach is required to optimize mechanical properties and degradation rate. These biodegradable stents offer a promising advantage over traditional metallic stents in that they dissolve completely in the body after a period, thus reducing long-term adverse effects such as restenosis. The ability to remove a foreign object from the body after treatment of an obstruction is especially attractive given current demographic trends, which indicate that people are living longer after a percutaneous coronary intervention procedure (Tabares Ocampo et al., 2023). Traditionally, biodegradable stents require a thicker strut compared to conventional stents due to the weaker nature of the degradable materials. However, a thicker strut leads to worse patient outcomes.

As mentioned in both cases, it is essential to consider the degradation of the medical device as an essential design variable. This degradation is not only dependent on the material and the environment, but also on the geometry of the device and must be in balance with tissue regeneration. The device must disintegrate completely once it has fulfilled its mechanical function. About this characteristic, the degradation of the material leads to a loss of properties that must be quantified. In some cases, this loss may be beneficial, while in others it may be detrimental. Therefore, controlling degradation ensures a stable mechano-biological response.

To estimate *in silico* how the calibrated model could aid in biodevice design, CT-like axial slices were generated using Chitubox[®] v1.9. 0 (Chitubox, Zhongcheng Future Industrial Park, Hangcheng Avenue, Baoan District, Shenzhen, Guangdong, China 518128) of a personalized coronary stent exposed in the study by (Solórzano-Requejo et al., 2023) and a tissue-engineered gyroid scaffold designed using the open-source software MS Lattice (Al-Ketan & Abu Al-Rub, 2021). Figure 6 shows the slice degradation process for each of the medical devices. By performing the conversion from iterations to time, considering that 68 iterations equal to approximately 400 minutes, the designer would be able to analyze whether the implant degrades in the right time frame and which areas are most prone to degrade rapidly. Moreover, this is achieved at a very low computational cost, as the CA model is very optimal in that aspect.

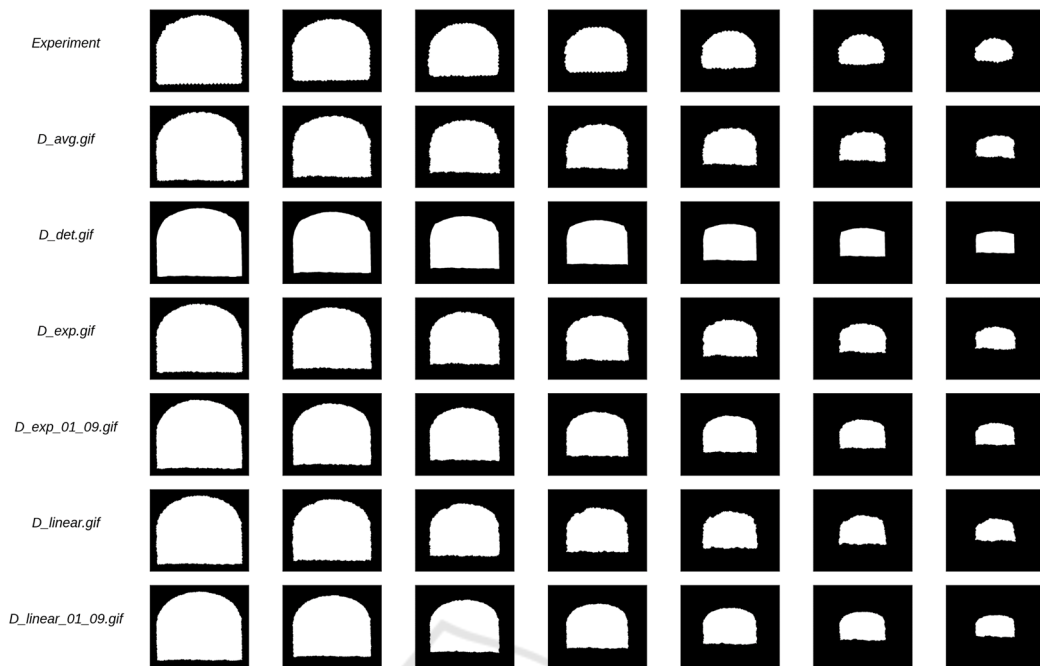


Figure 5: Comparison between experimental results and simulations with different rules for the D-shaped specimen.

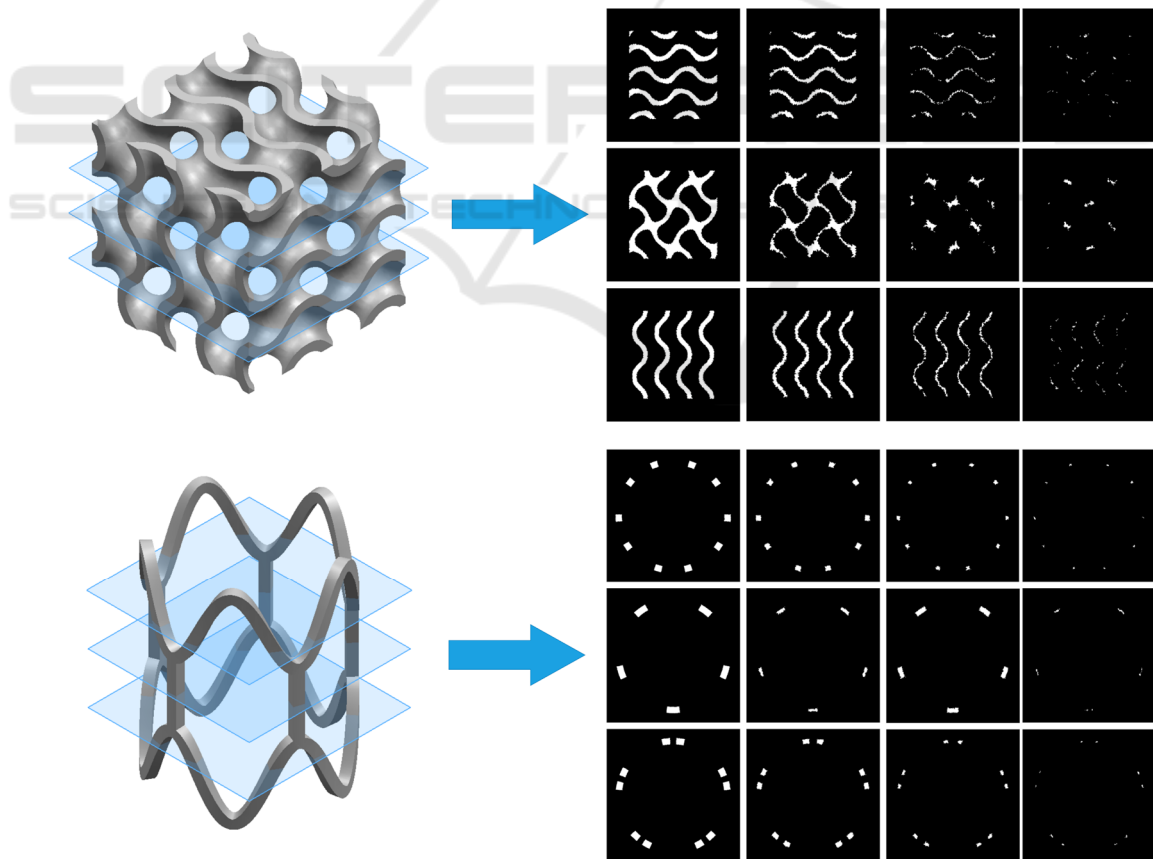


Figure 6: PCA simulation of axial slices of a tissue engineering scaffold and coronary stent.

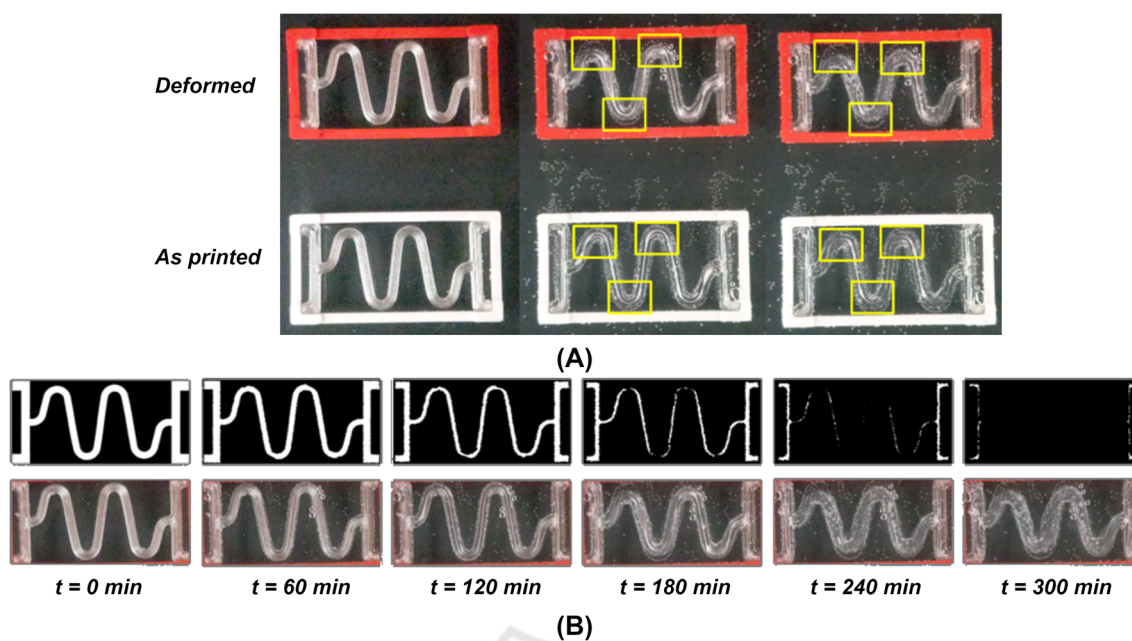


Figure 7: (A) Comparison of the degradation between two springs: one deformed by a framework during the degradation process and the other printed directly with the deformed shape. (B) Simulation using the CA whose rules are influenced by the stress state.

4 FUTURE PROPOSALS

In this study, a calibrated model capable of capturing the complex two-dimensional interactions in medical devices has been developed. However, to accurately assess the degradation of these devices, it is essential to adopt a three-dimensional perspective. By connecting this model to finite element software, it is possible to analyze how mechanical properties, such as stiffness and creep, are affected by the progressive degradation of the structure.

In the context of the mechanical state of the material, it is crucial to consider how stresses and strains impact the degradation rate. Therefore, it is possible to use information obtained from a structural analysis to define the rules of the CA model. These rules should not only depend on the neighborhood, but also on the stress state of the structure. More mechanically loaded areas will experience faster degradation compared to less stressed areas.

Additionally, in this study, experiments have been carried out with PVA serpentine springs, which serve as a prototype of implants for craniosynostosis, aiming to promote brain growth. To test the influence of the stress state, the degradation of two springs, one deformed by a frame during degradation and the other printed directly with the deformed shape obtained from the finite element software as an STL file, was

compared. The results were revealing: the degradation was noticeably more pronounced in the curved regions that were highly deformed. Then, the probabilities calibrated in our model were adjusted as a function of the deformation of the springs (Figure 7).

This finding suggests that it is possible to hybridize both methodologies, using a three-dimensional CA model within finite element software meshed with hexahedral elements. In this approach, each mesh element can represent a cell, and the degradation probabilities would depend on the specific stress state of each cell. This would allow accurate simulation of how the material behaves when the stress state varies, especially in biodegradable biomedical devices under varying loads.

5 CONCLUSIONS

This study presents a methodology for accurate simulation of two-dimensional biodegradable specimens, representing a significant advance in the accurate simulation of degradation in medical devices. Detailed results and meticulous comparisons of CA rules have revealed that the exponential rule

(R_{exp}) derived from Markov chains offers a highly reliable simulation of PVA degradation.

This approach not only deepens our fundamental understanding of degradation, which is influenced by material, environment, and part geometry, but also has practical applications in the design of biodegradable medical devices. By simulating devices such as coronary stent, tissue engineering scaffold and prototypes of implants for craniosynostosis, their degradation can be assessed *in silico*, providing valuable information for engineers and medical professionals.

In addition, this study has clearly pointed to future research directions. The adoption of a three-dimensional approach, integrating CA with finite element models, promises to offer even more accurate simulation, especially when considering the stress state of each cell. This hybrid approach could unlock new insights into how devices respond to different loads, essential for the design of devices that integrate optimally with the surrounding biological tissue.

ACKNOWLEDGEMENTS

This project has received funding from the European Union's Horizon Europe research and innovation programme under grant agreement No 101047008 (BIOMET4D). Views and opinions expressed are however those of the authors only and do not necessarily reflect those of the European Union or the European Innovation Council and SMEs Executive Agency (EISMEA). Neither the European Union nor the EISMEA can be held responsible for them.

REFERENCES

- Agapie, A., Andreica, A., & Giuclea, M. (2014). Probabilistic Cellular Automata. *Journal of Computational Biology*, 21(9), 699-708. <https://doi.org/10.1089/cmb.2014.0074>
- Al-Ketan, O., & Abu Al-Rub, R. K. (2021). MSLattice: A free software for generating uniform and graded lattices based on triply periodic minimal surfaces. *Material Design & Processing Communications*, 3(6). <https://doi.org/10.1002/mdp2.205>
- Ballesteros Hernando, J., Ramos Gómez, M., & Díaz Lantada, A. (2019). Modeling Living Cells Within Microfluidic Systems Using Cellular Automata Models. *Scientific Reports*, 9(1), 14886. <https://doi.org/10.1038/s41598-019-51494-1>
- Caselles, V., Kimmel, R., & Sapiro, G. (1997). Geodesic Active Contours. *International Journal of Computer Vision*, 22(1), 61-79. <https://doi.org/10.1023/A:1007979827043>
- Colafiglio, T., Lofù, D., Sorino, P., Festa, F., Di Noia, T., & Di Sciascio, E. (2023). Exploring the Mental State Intersection by Brain-Computer Interfaces, Cellular Automata and Biofeedback. *IEEE EUROCON 2023 - 20th International Conference on Smart Technologies*, 461-466. <https://doi.org/10.1109/EUROCON56442.2023.10198964>
- Dascălu, M. (2018). Cellular Automata and Randomization: A Structural Overview. En R. Lopez-Ruiz (Ed.), *From Natural to Artificial Intelligence—Algorithms and Applications*. IntechOpen. <https://doi.org/10.5772/intechopen.79812>
- Deutsch, A., & Dormann, S. (2017). *Cellular Automaton Modeling of Biological Pattern Formation*. Birkhäuser Boston. <https://doi.org/10.1007/978-1-4899-7980-3>
- Díaz Lantada, A., Urosa Sánchez, M., & Fernández Fernández, D. (2023). In silico Tissue Engineering and Cancer Treatment Using Cellular Automata and Hybrid Cellular Automata-Finite Element Models: Proceedings of the 16th International Joint Conference on Biomedical Engineering Systems and Technologies, 56-63. <https://doi.org/10.5220/0011742300003414>
- Gardner, M. (1970). *Mathematical Games*. *Scientific American*, 223(4), 120-123.
- Kalkhof, J., González, C., & Mukhopadhyay, A. (2023). Med-NCA: Robust and Lightweight Segmentation with Neural Cellular Automata. En A. Frangi, M. De Bruijne, D. Wassermann, & N. Navab (Eds.), *Information Processing in Medical Imaging (Vol. 13939, pp. 705-716)*. Springer Nature Switzerland. https://doi.org/10.1007/978-3-031-34048-2_54
- Liu, Y.-Y., Blazquez, J. P. F., Yin, G.-Z., Wang, D.-Y., Llorca, J., & Echeverry-Rendón, M. (2023). A strategy to tailor the mechanical and degradation properties of PCL-PEG-PCL based copolymers for biomedical application. *European Polymer Journal*, 198, 112388. <https://doi.org/10.1016/j.eurpolymj.2023.112388>
- Liu, Z., Fang, H., Xu, J., & Wang, K.-W. (2023). Cellular automata inspired multistable origami metamaterials for mechanical learning. <https://doi.org/10.48550/ARXIV.2305.19856>
- Solórzano-Requejo, W., Aguilar, C., Zapata Martínez, R., Contreras-Almengor, O., Moscol, I., Ojeda, C., Molina-Aldareguia, J., & Diaz Lantada, A. (2023). Artificial Intelligence and Numerical Methods Aided Design of Patient-Specific Coronary Stents: Proceedings of the 16th International Joint Conference on Biomedical Engineering Systems and Technologies, 37-45. <https://doi.org/10.5220/0011639000003414>
- Tabares Ocampo, J., Marín Valencia, V., Robledo, S. M., Upegui Zapata, Y. A., Restrepo Múnera, L. M., Echeverría, F., & Echeverry-Rendón, M. (2023). Biological response of degradation products of PEO-modified magnesium on vascular tissue cells, hemocompatibility and its influence on the inflammatory response. *Biomaterials Advances*, 154, 213645. <https://doi.org/10.1016/j.bioadv.2023.213645>
- Von Neumann, J., & Burks, A. W. (1966). Theory of self-reproducing automata. *IEEE Transactions on Neural Networks*, 5(1), 3-14.